PEA System Development for Measurement of Volume Charge Distributions in Thin Dielectric Films

Lee H. Pearson,[1] JR Dennison,[2] Erick W. Griffiths[1] and Anthony C. Pearson[1]

[1] Box Elder Innovations, LLC [2] Utah State University

I. Introduction

Pulsed Electro-Acoustic (PEA) measurement techniques are nondestructive and, arguably, one of the most promising methods to provide the desired information on internal charges distributions related to spacecraft charging issues [1,2].

This paper discusses an effort to develop advanced PEA system capabilities that incorporate:

- Improved signal processing tools for increased signal/noise ratios (SNR)
- Integrated PEA modeling tools

II. Improved Signal Processing

Signal processing methods developed in this program are described below, including averaging, band-pass filter, split spectrum processing, and deconvolution. These methods are not only helpful in reducing noise, but also in improving spatial resolution.

Waveform Averaging

Simple averaging of N waveforms reduces SNR by $\sqrt{N}$.

Band-Pass Filtering

$$Filter(f) = e^{-\frac{4\ln(2)}{BW^2}(f-f_0)^2} \sin\left(\frac{\pi}{2f_0} f\right)$$

Wiener Deconvolution [4]

$$X(\omega) = \frac{Y(\omega)H^*(\omega)}{|H(\omega)|^2 + Q^2|H(\omega)|^2_{\max}}$$

$X(\omega)$ = material response

$Y(\omega)$ = measurement

$H(\omega)$ = instrument response

Q = adjustible parameter

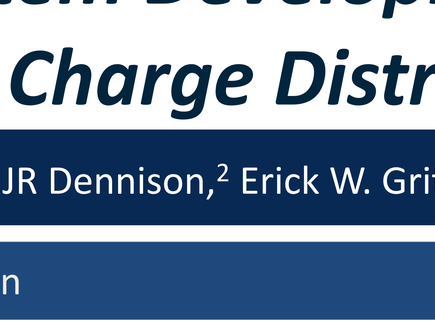

Figure 1. Flow Diagram Showing Signal Processing and Data Analysis Process

Split Spectrum Processing [3]

- Raw waveform Fourier transformed to frequency-domain and split into N wavelets using overlapping Gaussian band-pass filters
- Wavelets transformed back into time-domain
- For each element in the wavelets, the average and standard deviation are calculated from which the coefficient of variation (CV=stdev/avg) is calculated.
- Each element original waveform divided by corresponding CV

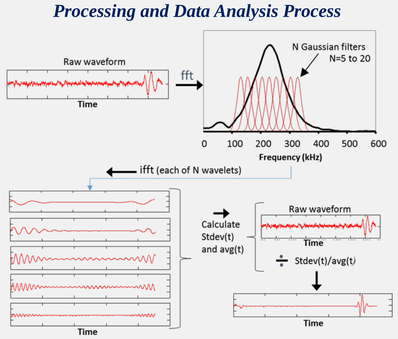

Figure 2. Graphical Representation of Split Spectrum Processing Method

III. PEA Modeling with Ray Tracing [1,5-15]

For a volume charge distribution, $\rho(z)$, in a dielectric layer, a force acts on the charge layer when an external pulsed electric field, $E(t)$, is applied. The force on a thin sub-layer of charge of thickness, Δz, at location z, is given by:

$$\Delta f(z,t) = \rho(z) \cdot \Delta z \cdot E(t) \quad (1)$$

In the frequency domain, this expression is written:

$$\Delta f(\omega, z) = \rho(z) \cdot \Delta z \cdot E(\omega) \quad (2)$$

where $\Delta f(\omega,z)$ and $E(\omega)$ are Fourier transforms of $\Delta f(z,t)$ and $E(t)$. The force (over the cross sectional area) creates a pressure wave that propagates to the piezoelectric sensor and is given by:

$$\Delta p(\omega, z) = p_0(\omega) \cdot \rho(z) \cdot \Delta z \cdot E(\omega) \cdot e^{ik_4 z} \cdot e^{ik_3 h_3} \cdot t_{43} \cdot t_{32} \quad (3)$$

where $p_0(\omega)$ is the transducer-instrumentation response function and is assumed to have a Gaussian response shape in frequency domain. t_{43} and t_{32} are the transmission coefficients for the dielectric film-electrode and electrode-piezoelectric sensor interfaces (refer to Fig. 3). Exponential factors are added to account for the phase shifts (or time delays in time domain) for each respective layer. The z-coordinate can be transformed to a time coordinate with the following substitutions:

$$z = t \cdot c_4 \; ; \; \Delta z = c_4 \Delta t \; ; \; k_4 = \frac{\omega}{c_4} \quad (4)$$

where c_4 is the wavespeed in the dielectric, ω is the angular frequency, and k_4 is the dielectric wavevector.

Eq. 3 can now be written:

$$\Delta p(\omega, t) = p_0(\omega) \cdot E(\omega) \cdot c_4 \cdot e^{ik_3 h_3} \cdot t_{43} \cdot t_{32} \cdot \rho(c_4 t) \cdot e^{i\omega t} \Delta t \quad (5)$$

Summing up all the wavelets from each charge sub-layer (Δz) is accomplished by integrating as follows:

$$p(\omega) = p_0(\omega) \cdot E(\omega) \cdot c_4 \cdot e^{ik_3 h_3} \cdot t_{43} \cdot t_{32} \cdot \int_0^t \rho(c_4 t) \cdot e^{i\omega t} \cdot dt \quad (6)$$

Setting the limits on the integral to +/- infinity changes the integral to a Fourier integral and Eq. 6 can now be written in terms of the Fourier transform of the charge distribution, $\rho(\omega)$:

$$p(\omega) = p_0(\omega) \cdot E(\omega) \cdot c_4 \cdot e^{ik_3 h_3} \cdot t_{43} \cdot t_{32} \cdot \rho(\omega) \quad (7)$$

Eq. 7 is the stress transferred to the sensor from the charge layer. The stress, σq, from the embedded charge in the dielectric layer is then given by

$$p(\omega) = E(\omega) \cdot c_4 \cdot \rho(\omega) = \sigma q \quad (8)$$

Mathematically, the time delay (phase shift) due to the z-dependence of the charge distribution integrates to $\rho(\omega)$. The time-domain waveform (shown in Fig. 3) is obtained by performing an inverse Fourier transform on $p(\omega)$ from Eq. 8 and then taking the real-part:

$$p(t) = \mathrm{Re}[icfft[p(\omega)]] \quad (9)$$

The derivation leading to Eqs. 7-9 is for the wave designated by p_{20} in Fig. 4. The wavelets p_{10} and p_{30}, for the waves generated from the induced charges on the electrodes can be written:

$$p_{10}(\omega) = p_0(\omega) \cdot E(\omega) \cdot e^{ik_3 h_3} \cdot t_{32} \quad (10)$$

$$p_{30}(\omega) = p_0(\omega) \cdot E(\omega) \cdot c_4 \cdot \rho(c_4\omega) \cdot e^{ik_3 h_3} \cdot t_{43} \cdot t_{32} \quad (11)$$

Other wavelets can be similarly derived. In general, there are an infinite number, but only a few are needed in practice.

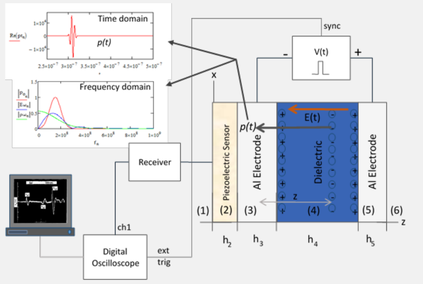

Figure 3 Conceptual diagram showing a generic PEA setup with a charged dielectric film, electrodes, sensor, and basic equipment components

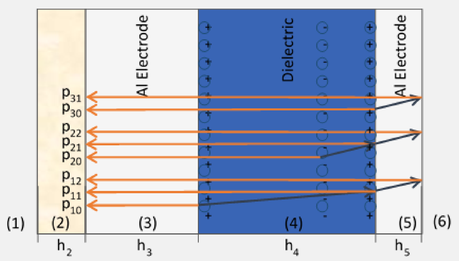

Figure 4 Drawing showing additional wavelets including additional reflecting wavelets and wavelets coming from induced charge layers

IV. Summary

In summary, signal processing and modeling tools have been developed, debugged, and proven out, and have been found to be beneficial in cleaning up waveforms (see Fig. 5) and analyzing their meaning and content.

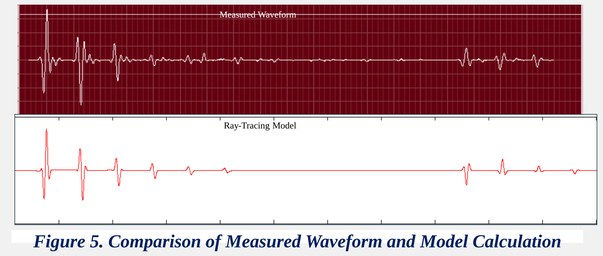

Figure 5. Comparison of Measured Waveform and Model Calculation

A prototype pulsed electro-acoustic (PEA) system using the signal processing and modeling tools has been designed, developed, built, and demonstrated for ambient environmental conditions. Work is underway on development of a vacuum chamber-based PEA system. Both the ambient and vacuum chamber-based systems use the same LabVIEW data acquisition, instrument control, signal processing and analysis, and modeling package.

References

1. Arnaout, M., Berquez, L., Baudoin, F., and Payan, D., (2010). Contribution to Improving the Spatial Resolution of a Pulsed Electro Acoustic Cell Measurement, *IEEE Int. Conf. Solid Dielectrics*, Germany.
2. Dennison, J.R. & Pearson, L.H. "Pulse Electro-Acoustic (PEA) Measurements of Embedded Charge Distributions," (2013). *Proc. SPIE Optics and Photonics Conf.*, 8876, 887612-1-887612-11
3. Newhouse, V.L., et.al., (1982). Flaw-to-Grain Echo Enhancement by Split-Spectrum Processing, *Ultrasonics*, Mar, p. 59.
4. Honarvar, F., et.al., (2004). A New Signal Processing Technique for Enhancement of Ultrasonic Testing Signals, *Proc. World Conf. on NDT*, Montreal, Canada.
5. Griseri, V., *et. al.*, (2004). Pulsed Electro-Acoustic Technique Applied to *In-situ* Measurement of Charge Distribution in Electron-irradiated Polymers, *IEEE Trans. Dielectrics and Electrical Insulation*, 11(5), 891.
6. Laurenceau, P., Dreyfus, G., and Lewiner, J., (1977). New Principle for the Determination of Potential in Dielectrics, *Phys. Rev. Lett*. 38(1), 46.
7. Sessler, G. M., West, J. E., Berkley, D. A., and Morgenster, G., (1977). Determination of Spatial Distribution of Charges in Thin Dielectrics, *Phys. Rev. Lett*. 38(7), 368.
8. Gallot-Lavallée, O., Griseri, V., Teyssedre, G., and Laurent, C., (2005). The Pulsed Electro-Acoustic Technique in Research on Dielectrics for Electrical Engineering: Today's Achievements and Perspectives for the Future, *RS - RIGE*. 8(5-6), 749.
9. Griseri, V., Boucharеb, S., Berquez, L., (2012). Adaptation of the LIMM Technique Data Treatment to Perform Measurements in Vacuum, *2012 IEEE Conf. on Electrical Insulation and Dielectric Phen. (CEIDP)*, Montreal,, Canada,
10. Miyake, H., Numata, S., Tanaka, Y., and Takada, T., (2010). Characteristic of Internal Charge Distribution in PI Irradiated by Proton, *10th Spacecraft Charging Tech. Conf.*, Albuquerque, NM.
11. Griseri, V., *et. al.*, (2006). Space-Charge Detection and Behavior Analysis in Electron-irradiated Polymers, *IEEE Trans. Plasma Sci.*, 34(5), 2185.
12. Maeno, T., *et. al.*, (1988). Measurement of Spatial Charge Distribution in Thick Dielectrics Using the Pulsed Electroacoustic Method, *IEEE Trans. Electrical Insulation*, 23(3), 433.
13. Takada, T., et.al., (1998). Comparison Between the PEA Method and the PWP Method for Space Charge Measurement in Solid Dielectrics, *IEEE Trans. on Dielectrics and Electrical Ins.*, 5(6), 944.
14. Takada, T., Miyake, H., and Tanaka, Y., (2006). Pulse Acoustic Technology for Measurement of Charge Distribution in Dielectric Materials for Spacecraft, *IEEE Trans. on Plasma Science*, 34(5), 2176.
15. Tashima, D., Kurosawatsu, K., Sung, Y-M., Otsubo, M., and Honda, C., (2007). Surface Modification of Nanoporous Materials for Electric Double Layer Capacitors Application, *Materials Chemistry and Physics*, 103(1), 158.

This work was supported by Small Business Technology Transfer Research (STTR) Phase I and Phase II funding from the Air Force Research Laboratory, Kirtland AFB, Albuquerque, NM, USA.

Lee Pearson
Box Elder Innovations, LLC
Bear River City, Utah
Lee.Pearson@boxelderinnovations.com

JR Dennison
Utah State University
Physics Department
JR.Dennison@usu.edu

Scan QR code to access additional publications.